Publications

Available Online

J. Sci. Res. **13** (2), 361-375 (2021)

JOURNAL OF SCIENTIFIC RESEARCH

www.banglajol.info/index.php/JSR

Effect of Different Forms of Periodic Piecewise Linear Forces on Duffing Oscillator

S. V. Priyatharsini[1], B. Bhuvaneshwari[1], V. Chinnathambi[1*], S. Rajasekar[2]

[1]Department of Physics, Sadakathullah Appa College (Affiliated to Manonmaniam Sundaranar University), Tirunelveli-627 011, Tamilnadu, India

[2]School of Physics, Bharathidasan University, Tiruchirapalli 620 024, Tamilnadu, India

Received 2 October 2020, accepted in final revised form 28 January 2021

Abstract

The paper highlights the effect of different forms of periodic piecewise linear forces in the ubiquitous Duffing oscillator equation. The external periodic piecewise linear forces considered are Triangular, Hat, Trapezium, Quadratic and Rectangular. With the aid of some numerical simulation tools such as bifurcation diagram, phase portrait and Poincare´ map, the different routes to chaos and various strange attractors are found to occur due to the applied forces. The effect of an ε-parametric control force in the Duffing system is also analyzed. To characterize the regular and chaotic behaviors of this system, the maximal Lyapunov exponent is employed.

Keywords: Duffing oscillator; Piecewise linear force; Routes to chaos; Strange attractors; Chaos.

doi: http://dx.doi.org/10.3329/jsr.v13i2.49503 J. Sci. Res. **13** (2), 361-375 (2021)

1. Introduction

In the past, the study on the effect of different forms of smooth periodic forces has received much attention. Recent studies have shown that the effect of various smooth periodic forces on some nonlinear systems is significant and they can alter the dynamical behaviors drastically [1-10]. The study of such smooth periodic forces may help to select the appropriate external drive to generate and control nonlinear behaviors in some nonlinear systems. Duffing oscillator, named after Georg Duffing [11], is a famous damped and forced nonlinear dynamical system. Duffing oscillator equation represents a second-order ordinary differential equation with cubic nonlinearity and periodic excitation. From the last century, the Duffing-type nonlinear dynamical systems have been investigated uninterruptedly in various fields conducted by plenty of researches, such as physics, engineering, chemistry, economics and biological and social sciences [12-20]. The effect of smooth single or multiple forces has been studied extensively in Duffing oscillator [12,13,21-25]. Very few researchers reported about the applications of piecewise periodic linear forces [26-28]. Compared to harmonic forces, these forces are

* *Corresponding author*: veerchinnathambi@gmail.com

effectively used to stabilize some nonlinear systems with a relatively low frequency of fast oscillations. Up to now, a variety of control methods to achieve chaos control have been introduced in control theory such as parametric modulation [26], active control [29], adaptive control [30], backstepping design [31], feedback control [32], sliding mode control [33], impulsive control [34], etc. In this study, we also address the problem of chaos suppression by an ε-parametric control force defined for one of the periodic piecewise linear forces, which is less studied in the present literatures.

Motivated by the above, in the present paper we numerically study the effect of different forms of periodic piecewise linear forces in the Duffing oscillator equation.

$$\ddot{x} + a\dot{x} - \omega_0^2 x + \beta x^3 = F(t), \quad \alpha > 0 \tag{1}$$

Here, α is the damping coefficient, ω_0 is the natural frequency and β is the constant parameter which plays the role of nonlinear parameter. $F(t)$ is an external time dependent periodic driving force.

The potential of the Duffing oscillator is given by

$$V(x) = -\frac{1}{2}\omega_0^2 x^2 + \frac{1}{4}\beta x^4. \tag{2}$$

Depending on the set of the parameters, it can be considered at least three physically interesting situations where the potential is (i) single-well (ii) double-well and (iii) double hump potential well and are shown in Fig. 1. Each one of the above three cases has become a central point to describe inherently nonlinear phenomena, exhibiting a rich and variety of nonlinear behaviors. Throughout this paper, our analysis is of the double-well case. The symmetric double-well potential energy $V(x)$, which is a characteristic of this system, is drawn in Fig. 1b. The system (1) for the double-well potential has been studied by Holmes *et al.* [35] since 1979 and was derived as a mathematical model for a buckled beam or plasma oscillations, among others.

The paper is well organized as follows. In Section 2, we have presented the mathematical representation of different forms of periodic piecewise linear forces. In Section 3, we have analyzed the period-doubling cascades and strange attractors of the system (1) due to the applied periodic piecewise linear forces. In Section 4, we study the occurrence of bifurcations and chaos in the system (1) driven by an ε − parametric control periodic piecewise linear force. Finally, Section 5 sums up with the concluding remarks.

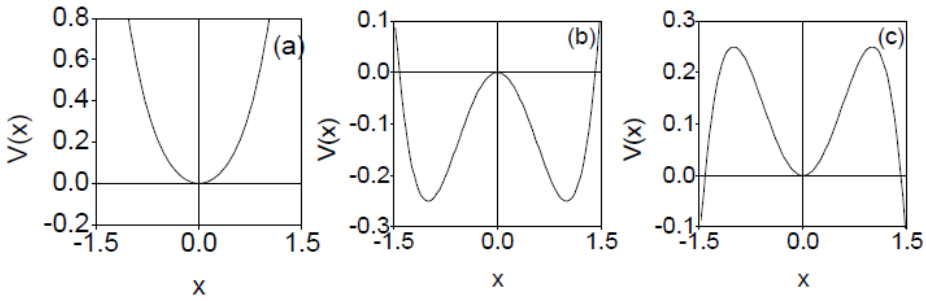

Fig. 1. Shape of the potential function of the Duffing system for (a) $\omega_0^2 < 0$, $\beta > 0$, (b) $\omega_0^2 > 0$, $\beta > 0$ and (c) $\omega_0^2 < 0$, $\beta < 0$.

2. Different Forms of Periodic Piecewise Linear Forces

The piecewise forces are ramped up (or down) over a short duration of time and held constant thereafter. Piecewise periodic linear forces such as triangular, trapezium and rectangular wave type forces can be used directly as an external force because these forces can be easily generated from the currently available waveform generator or op-amp or 555 timers. Hat type piecewise force is formed when a sine function is traced by a linear pulses and Quadratic type piecewise linear force is formed when the slopes are removed from the sine function at the beginning and end. Therefore, these two forces cannot be generated using the waveform generator or an op-amp or 555 timer. But one can construct the mathematical model equation for such piecewise forces and the output of the model system can be used as an external force. Fig. 2 shows different forms of periodic piecewise linear forces. The period T of all the forces considered in our study is fixed as $2\pi/\omega$. In particular, Ahamed [26] studied the stabilization of the pendulum system driven by these periodic piecewise forces with low frequency as compared to harmonic force. The mathematical forms of periodic piecewise linear forces are as follows.

2.1. *Triangular type force*

The mathematical form of triangular type force (Fig. 2a) is

$$F(t) = \begin{cases} \frac{4ft}{T}, & 0 \le t < \frac{T}{4} \\ -\frac{4ft}{T} + 2f, & \frac{T}{4} \le t < \frac{3T}{4} \\ \frac{4ft}{T} - 4f & \frac{3T}{4} \le t < T \end{cases} \tag{3}$$

where t is taken as mod $(2\pi/\omega)$.

2.2. *Hat type force*

The Hat type force (Fig. 2b) is represented by

$$F(t) = \begin{cases} \frac{f}{2}, & 0 \le t < \frac{T}{6} \\ f, & \frac{T}{6} \le t < \frac{T}{3} \\ \frac{f}{2}, & \frac{T}{3} \le t < \frac{T}{2} \\ -\frac{f}{2}, & \frac{T}{2} \le t < \frac{2T}{3} \\ -f, & \frac{2T}{3} \le t < \frac{5T}{6} \\ -\frac{f}{2}, & \frac{5T}{6} \le t < T \end{cases} \tag{4}$$

2.3. *Trapezium type force*

The mathematical representation for the Trapezium type force (Fig. 2c) is

$$F(t) = \begin{cases} \frac{8f}{T}, & 0 \le t < \frac{T}{8} \\ f, & \frac{T}{8} \le t < \frac{3T}{8} \\ \frac{8f}{T}\left(\frac{T}{2} - t\right), & \frac{3T}{8} \le t < \frac{5T}{8} \\ -f, & \frac{5T}{8} \le t < \frac{7T}{8} \\ \frac{8f(t-T)}{T}, & \frac{7T}{8} \le t < T \end{cases}, \tag{5}$$

2.4. *Quadratic type force*

The mathematical expression for the Quadratic type force (Fig. 2d) is

$$F(T) = \begin{cases} f, & 0 \le t < \frac{3T}{8} \\ \frac{8f}{T}\left(\frac{T}{2} - t\right), & \frac{3T}{8} \le t < \frac{5T}{8} \\ -f, & \frac{5T}{8} \le t < T \end{cases} \tag{6}$$

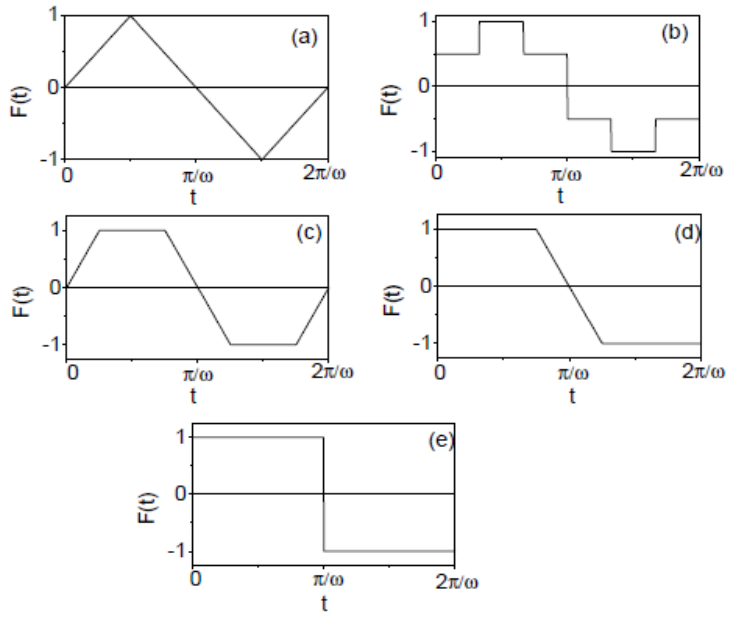

Fig. 2. Form of various periodic piecewise linear forces (a) Triangular, (b) Hat, (c) Trapezium, (d) Quadratic and (e) Rectangular waves. For all the forces period is $2\pi/\omega$, $\omega = 1$ and amplitude f is 1.0.

2.5. *Rectangular type force*

The mathematical representation for the Rectangular type force (Fig. 2e) is

$$F(T) = \begin{cases} f, & 0 \le t < \frac{T}{2} \\ -f, & \frac{T}{2} \le t < T \end{cases} \tag{7}$$

In the absence of external forcing term, the potential wells are stationary. When the system (1) is subjected to external periodic force $F(t)$, the potential has an additional term $-xF(t)$ (since $F = -\frac{\partial V}{\partial x}$). When the forcing amplitude f is small, the particles are oscillating within the wells. When the amplitude f of the excitation is large enough, the particle can escape from one of the potential wells into the other in a highly complex and random like fashion. As an example, the oscillatory behaviour of the potential during one drive cycle, (that is, at $t = 0, T/4, T/2, 3T/4, T$) for various periodic piecewise linear forces is shown in Fig. 3. The differences in the oscillatory behaviour of the potential wells due to the piecewise linear forces are clearly seen in the Fig. 3. For Hat type force, only asymmetric variation of the potential wells occur which is clearly evident in Fig. 3. The potential $V(x)$ given by Eq. (2) has two minima one in each of the potential wells and one maxima at the origin. We consider minima of the potential wells V_- and V_+ and the maximum between these two wells (Fig. 1b). We denote the location of the minima of the wells V_- and V_+ as x_-^* and x_+^* and the values of V at these minima as (V_-^{min}, V_+^{min}) respectively. The maximum between these two minima is denoted as (x*max) and the value of V at this maximum as V^{max}. The barrier heights from V_- to V_+ and V_+ to V_- denoted as h_- and h_+ respectively are

$$h_- = V^{max} - V_-^{min}, \qquad h_+ = V^{max} - V_+^{min} \tag{8}$$

The variation of the barrier heights h_- (dotted curve) and h_+ (continuous curve) as a function of t for all the periodic piecewise linear forces is shown in Fig. 4. The symmetric oscillations of the potential wells V_- and V_+ and the symmetric variations of the barrier heights of the wells h_- and h_+ are responsible for the nonlinear dynamics of the system (1). From Figs. 3 and 4, we found that for all the forces, the asymmetric variation of the potential wells and barrier heights are observed. Complex dynamical behaviors occur in the system (1) due to the asymmetric variation of the potential wells and barrier heights.

3. Period-Doubling Cascades and Strange Attractors

In the present work, we have used some effective numerical tools, such as, bifurcation diagram, the largest Lyapunov exponent, phase portrait and Poincare´ map to study the period- doubling cascades and strange attractors of the system (1). Eq. (1) involves five independent parameters $f, \alpha, \beta, \omega_0^2$ and ω.

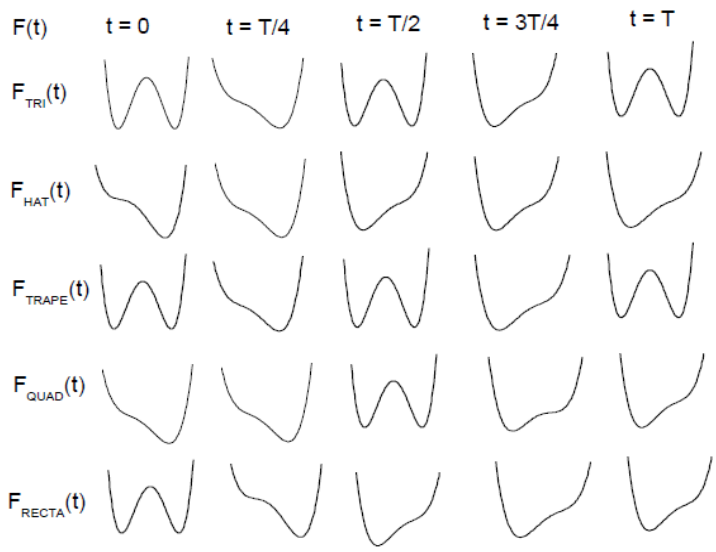

Fig. 3. Oscillatory behaviour of the potential at $t = 0, T/4, T/2, 3T/4$ and T for different periodic piecewise linear forces.

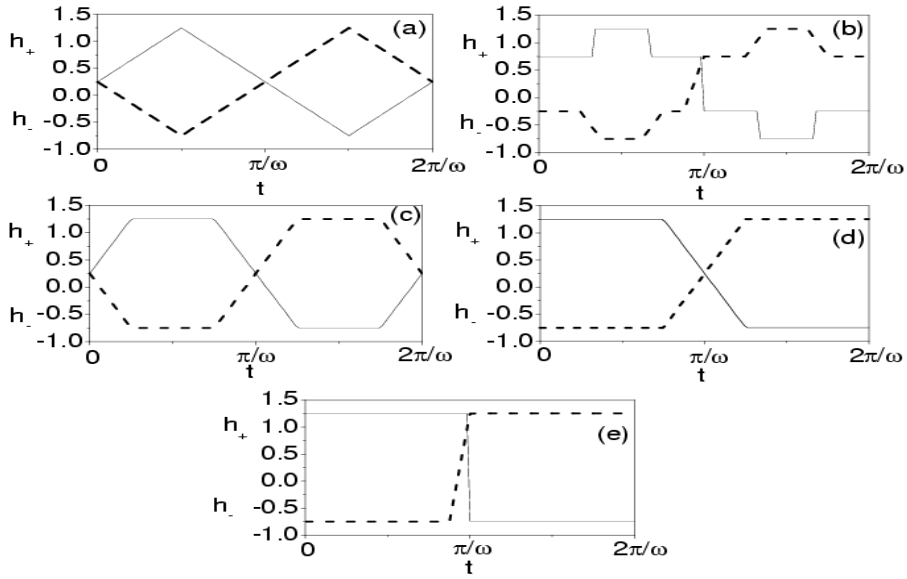

Fig. 4. Variation of the barrier heights h_- (dotted curve) and h_+ (continuous curve) as a function of t for the forces (a) Triangular, (b) Hat, (c) Trapezium, (d) Quadratic and (e) Rectangular waves. For all the forces period is $2\pi/\omega$, $\omega = 1$ and amplitude f is 1.0.

To simplify the analysis, all the parameters are kept constant except one to be varied. Here we choose f as bifurcation parameter. Now we fix $\omega_0^2 = 1$, $\alpha = 0.5$, $\beta = 1$, $\omega = 1$ and

let f to change in a wide range. The initial value in the numerical calculations are fixed at $x(0) = 1.0$ and $y(0) = 0.0$. Eq. (1) with different periodic piecewise linear forces are integrated by the fourth order Runge Kutta method with step size $(2\pi/\omega)/200$, where ω is the period of the driving forces. Numerical solution corresponding to first 500 drive cycles is left as transient. Fig. 5 shows the bifurcation diagrams and the corresponding maximal Lyapunov exponent (λm) for various periodic piecewise linear forces. We numerically calculated the maximal Lyapunov exponent (λ_m) employing Wolf *et al*. [36] algorithm. As expected, λ_m is negative in the periodic regime, ≈ 0 at bifurcation and positive in the chaotic regime. In order to gain some better insight of period-doubling and strange attractor features, magnification of a part of bifurcation diagrams is shown in Fig. 6. When the forcing amplitude f is varied, we can clearly notice many similarities and differences in the bifurcation dynamics. Consider the effect of triangular type force in the system (1), for small values of f, two period-T (= $2\pi/\omega$) orbits coexist, one in each potential well of the system. At $f = f_c = 0.396730$, a transcritical bifurcation occurs at which $\lambda \approx 0$. When the triangular type force is replaced by other types of periodic piecewise linear forces, similar behaviour is found to occur. Critical values of the transcritical bifurcation for other forces are given in Table 1. From Table 1, transcritical bifurcation occurs relatively earlier in the case of triangular type force whereas it is very much delayed by the quadratic type force. At $f = 0.431396$, the period-T orbit becomes unstable and gives birth to a period-2T orbit. Further increase in the value of f leads to successive bifurcation in the period-4T, 8T and 16T orbits are found to occur at $f = 0.4454692$, 0.449170 and 0.450157 and which is accumulated at $f = 0.450192$ where the onset of chaos is observed. When the triangular force is replaced by other forces, such as, hat, trapezium, quadratic and rectangular types of forces, similar behaviors are found to occur. The critical values of period-doubling bifurcations for all the forces are presented in Table 1.

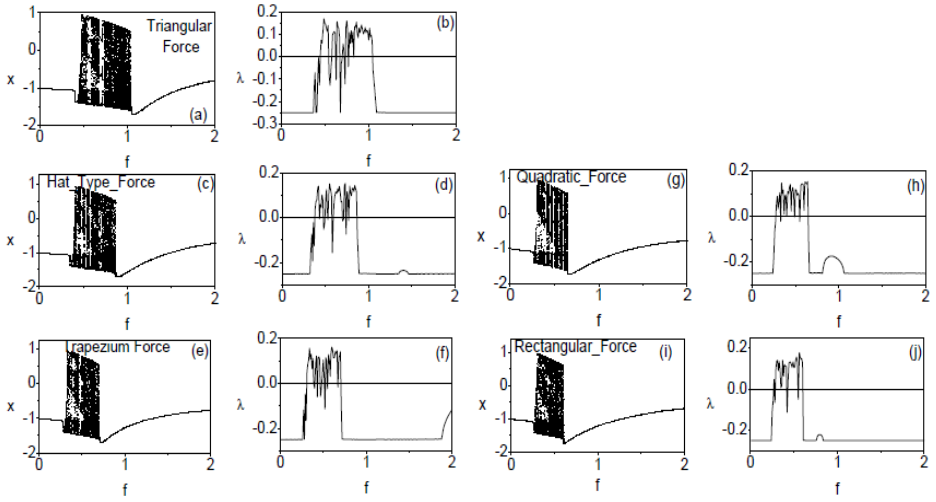

Fig. 5. Bifurcation diagrams and the corresponding maximal Lyapunov exponent diagrams of Duffing oscillator (Eq. 1) driven by various periodic piecewise linear forces.

Fig. 7 shows the Poincare´ maps of one band chaotic attractor at the accumulation of period-doubling phenomena. The geometrical structure of the attractor is different for various forces. In Table 1, we give the critical values of f at which various bifurcations occur for different forms of periodic piecewise linear forces. After the system becomes chaotic, a number of periodic windows, intermittent chaos, bifurcations of chaos which include band-merging, sudden-widening and sudden destruction behaviours appear. This type of behaviors is observed for all the forces. The critical values of all these bifurcations are presented in Table 1. In between the onset of chaos and band-merging crisis a periodic window region occurs. When the applied force is triangular type for f values just above f_c = 0.453550364, a period-8T orbits occur. When the forcing amplitude is decreased from f_c = 0.453550364, intermittent dynamics is developed. Laminar region with the unstable period-8T interrupted by chaotic burst is observed. The period of the orbit in the laminar is found to be different for other forces. For the forces such as hat and quadratic types, the period of the orbit in the laminar region is 5T while for the forces namely trapezium and rectangular types, the period is 6T .

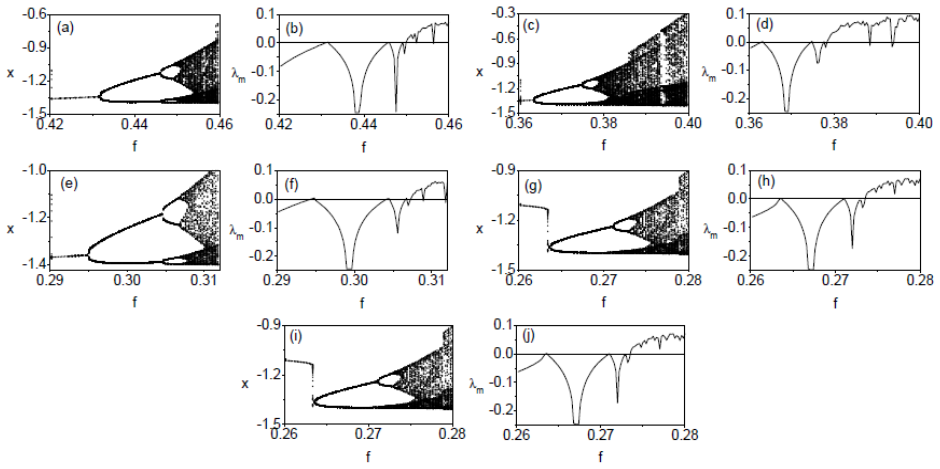

Fig. 6. Magnification of a part of bifurcation diagrams in Fig. 5. (a-b) Triangular, (c-d) Hat, (e-f) Trapezium, (g-h) Quadratic and (i-j) Rectangular forces.

For small values of f, the orbits confined to left-well alone and right-well alone exist for all the forces. But for higher values of f, the size of the orbit increases and at a critical value of f, cross-well motion is initiated for all the forces. At the critical values of forcing amplitude of cross-well motion, the chaotic orbits confined to each well potential joined together forcing a double-band chaotic attractor. For example, Fig. 8 shows the phase portraits and Poincare´ maps at the cross-well chaos for various forces. For all the forces, from a certain f values, the long-time motion settles to a periodic behaviour. Critical values of f at which the cross-well period-T occur for triangular, hat, trapezium, quadratic and rectangular type of forces are f = 1.08932, 0.867286, 0.720054, 0.657220 and 0.603957 respectively. Fig. 9 shows the phase portraits of cross-well period-T orbit for all the forces. Cross-well period-T orbit is realized for all the forces.

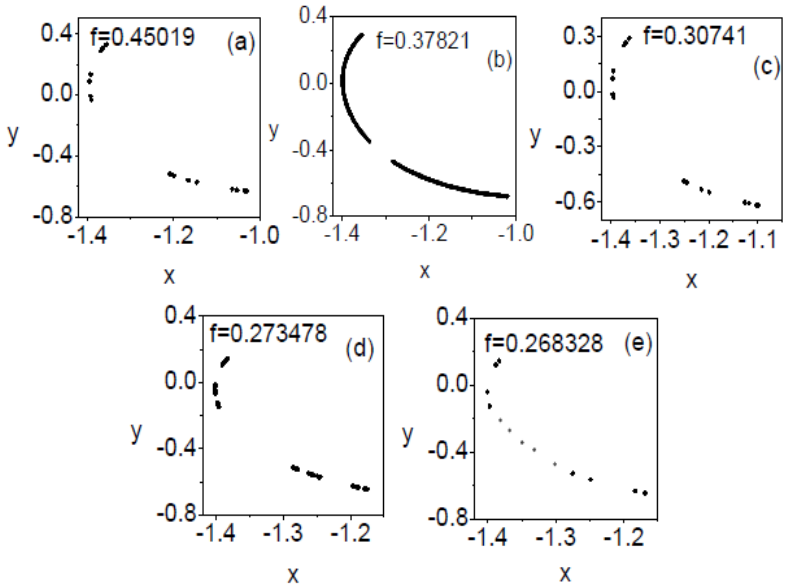

Fig. 7. Poincarémaps at the onset of chaos for various periodic piecewise linear forces (a) Triangular, (b) Hat, (c) Trapezium, (d) Quadratic and (e) Rectangular forces.

Table 1. Summary of bifurcation phenomena of the double-well Duffing oscillator (Eq. 1) driven by various periodic piecewise forces with α=0.5, β=1, ω_0^2=1 and ω=1.

Bifurcations	Critical values of amplitude of the various periodic piecewise forces				
	Triangular	Hat	Trapezium	Quadratic	Rectangular
Transcritical	0.396730	0.345634	0.279172	0.263276	0.258262
Period-2T	0.431396	0.365158	0.294128	0.263429	0.265745
Period-4T	0.445492	0.374587	0.304315	0.271179	0.267690
Period-8T	0.449170	0.377443	0.306709	0.272860	0.268118
Period-16T	0.450157	0.377756	0.306950	0.273252	0.268281
Onset of chaos	0.450192	0.378206	0.307413	0.273478	0.268363
Band-merging	0.454100	0.381534	0.310852	0.273949	0.270444
Sudden widening	0.459148	0.406101	0.329643	0.305852	0.291712
Intermittency	0.453550	0.383298	0.311596	0.276844	0.271667
Cross-well period-T	1.08932	0.867286	0.720054	0.657220	0.603957

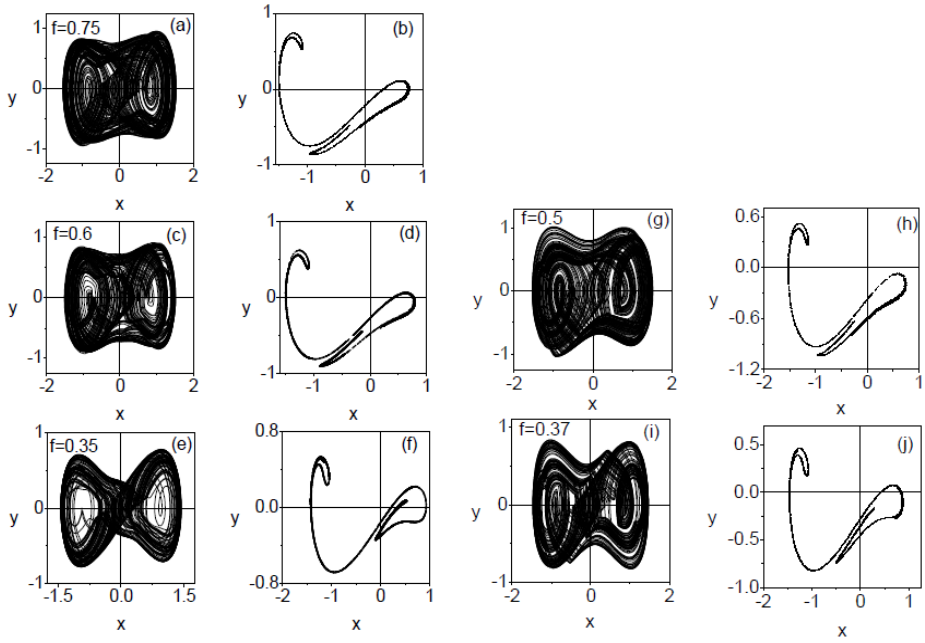

Fig. 8. Phase portraits and Poincare´ maps at the cross-well chaos for various periodic piecewise linear forces (a) Triangular, (b) Hat, (c) Trapezium, (d) Quadratic and (e) Rectangular

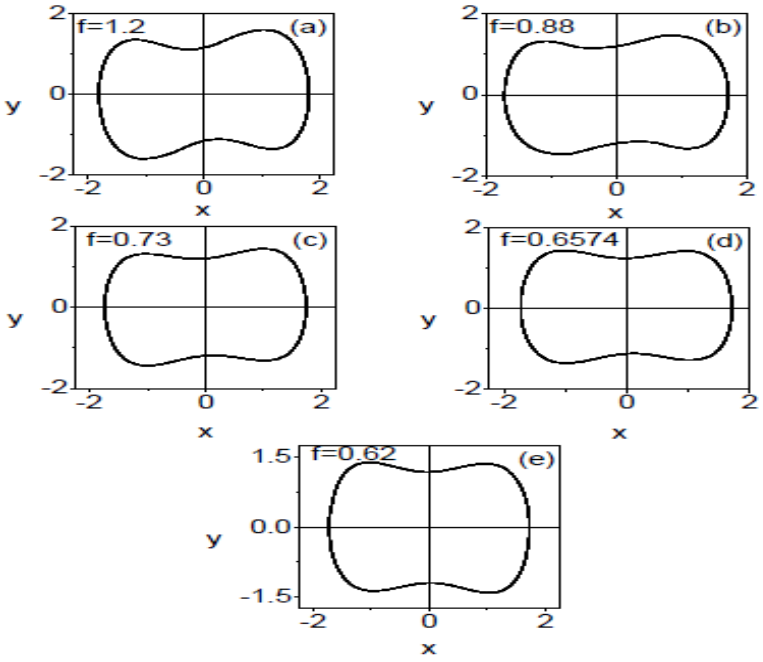

Fig. 9. Phase portraits of the system (1) at the cross-well period-T orbit for various periodic piecewise linear forces (a)Triangular, (b) Hat, (c) Trapezium, (d) Quadratic and (e) Rectangular.

4. Bifurcations and Chaos due to ε-Parametric Control Force

In the previous section, we studied the occurrence of period-doubling cascades and strange attractors in the system (1) driven by non-parametric control periodic piecewise linear forces. In this section, we study the occurrence of bifurcation and chaos in the system (1) driven by an ε-parametric control periodic piecewise linear force. An ε-parametric control is defined for one of the periodic piecewise linear forces. This ε-parametric force with $0 < \varepsilon < 1$ is given by (similar to the Quadratic type force (Eq. 6),

$$F(T) = \begin{cases} f, & 0 \le t < \frac{1-\epsilon}{2}T \\ \frac{f}{\epsilon}\left(-\frac{2}{T}+1\right), & \frac{1-\epsilon}{2}T \le t < \frac{1+\epsilon}{2}T \\ -f, & \frac{1+\epsilon}{2}T \le t < T \end{cases} \tag{9}$$

and is illustrated in Fig. 10 for three values of ε, namely, ε = 0.17, 0.5 and 0.9. From Fig. 10, it is clearly observed that when ε = 0.17, the curve of quadratic type force approaches the rectangular type force curve.

The bifurcation diagrams and the corresponding largest Lyapunov exponents of the system (1) driven by an ε-parametric force for three values of ε, namely, ε = 0.17, 0.5, 0.9 are shown in Fig. 11. The effect of ε can be clearly seen in the bifurcation diagrams (Fig. 11). For ε = 0.17, the bifurcation structure is identical with the bifurcation structure of rectangular force. This is clearly evident in Figs.11a and 5a. In order to gain some better insight of various bifurcations, chaos and strange attractor features are also shown in the bifurcation diagrams Fig. 12, which is the magnification of a part of bifurcation diagram Fig. 11. In Fig. 11a, as f is increased from 0, a stable period-T orbit occurs which persists up to f_c = 0.261185 and then it loses its stability giving birth to a period-doubling cascades and chaotic orbits. When the parameter f further increases from f_c one finds that the chaotic orbits persists for a range of f values interspersed periodic windows, period-doubling windows and intermittency route to chaos. At f = 0.599758, the chaotic motion suddenly disappears and the long-time motion settles to a periodic motion. The bifurcation structures and the corresponding largest Lyapunov exponents for ε = 0.5 and 0.9 are shown in Figs. 11(c-d) and (e-f). These Figures confirm the existence of period doubling cascades and strange attractors for ε = 0.5 and 0.9. In Fig. 11(c-d), period-T orbits occurs when ε < 0.280532. Period doubling cascades and strange attractors occur in the region $0.280532 < f < 0.802902$. When f > 0.802902 the long-time motion settles to a period-T orbit. Similarly, for ε = 0.9, period-T orbit occurs when f < 0.396614 and in the region $0.396614 < f < 1.151148$, period-doubling cascades and chaos occur. Cross-well period-T occurs when f > 1.151148. Due to the excitation of this force in the system (1) suppression of chaos is found for certain range of values of the control parameter f. This is clearly evident in Fig. 12.

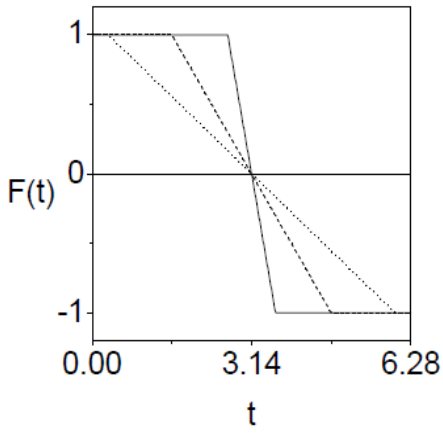

Fig. 10. Form of ε–parametric control periodic piecewise force for three values of ε, namely, ε = 0.17, 0.5 and 0.9.

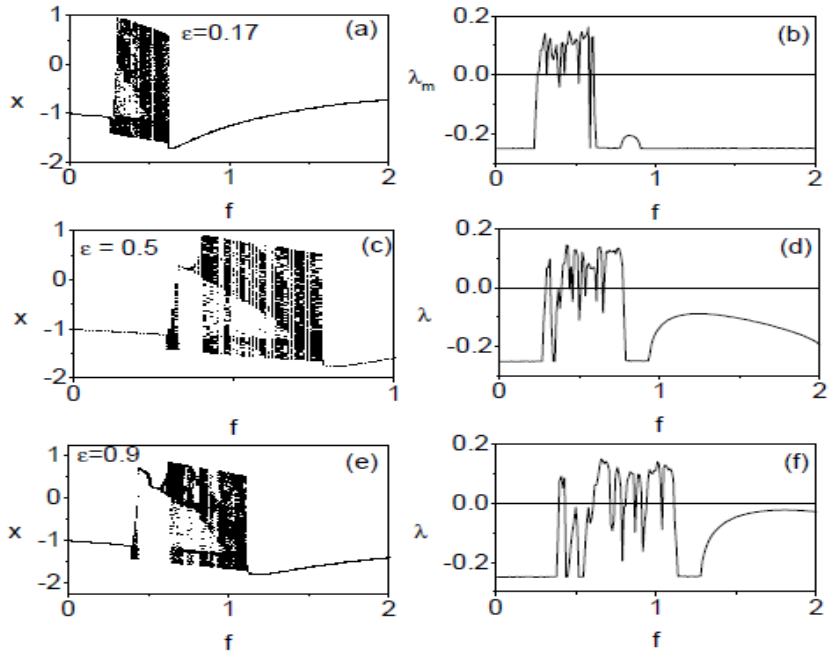

Fig. 11. Bifurcation diagrams and the corresponding maximal Lyapunov exponent diagrams of Duffing oscillator (Eq. 1) driven by an ε-parametric periodic piecewise linear force for three values of ε.

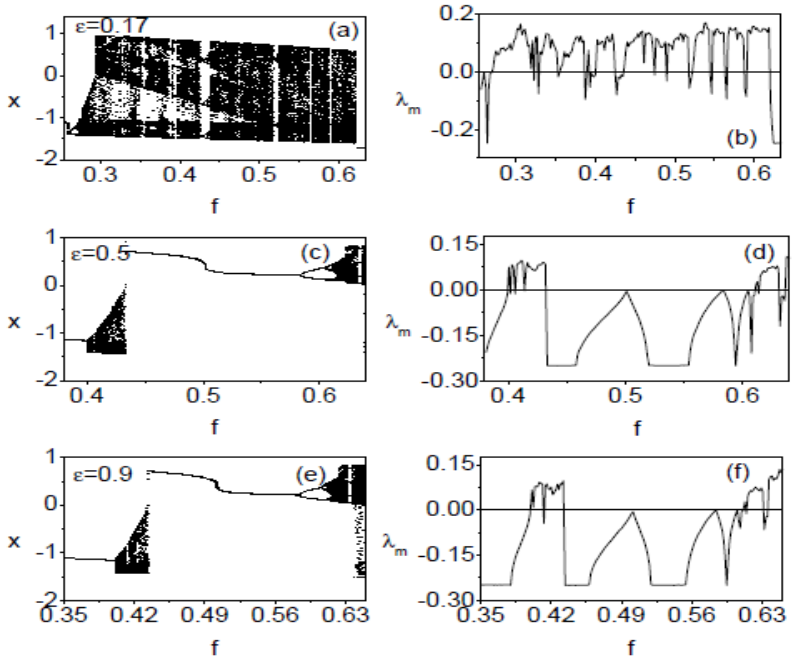

Fig. 12. Magnification of a part of bifurcation diagrams in Fig. 11.

5. Conclusion

In the present paper, we have carried out a preliminary numerical study on the effect of different forms periodic piecewise linear forces in the ubiquitous Duffing oscillator equation. For our numerical study, we fixed the period of the forces as $2\pi/\omega$ and $\omega = 1.0$. For a particular set of values of the parameters, we have shown the occurrence of period-doubling cascades and strange attractors and noticed many similarities and differences in the bifurcation structures due to the applied forces. Bifurcations and chaos of the system is also analyzed by an ε-parametric control force. Suppression of chaos is found for certain range of values of the control parameter f due to the ε-parametric control force. It is important to study the various nonlinear phenomena including resonance, hysteresis, vibrational resonance and stochastic resonance in the presence of different forms periodic piecewise linear forces. These will be investigated in future study.

References

1. J. Guckenheimer and P. Holmes, Nonlinear Oscillations, Dynamical Systems and Bifurcations of Vector Fields (Springer-Verlag, New York, 1987).
2. R. Chacon, J. Math. Phys. **38**, 1477 (1997). https://doi.org/10.1063/1.531816
3. K. Konishi, Phys. Lett. A **320**, 200 (2003). https://doi.org/10.1016/j.physleta.2003.11.024

4. Z. M. Ze and W.Y. Leu, Chaos, Solitons Fractals **20**, 503 (2004). https://doi.org/10.1016/j.chaos.2003.07.001
5. Y. C. Lai, Z. Liu, A. Nachman, and L. Zhu, Int. J. Bifur. Chaos **14**, 3519 (2004). https://doi.org/10.1142/S0218127404011454
6. V. M. Gandhimathi, K. Murali, and S. Rajasekar, Chaos, Solitons Fractals **30**, 1034 (2006). https://doi.org/10.1016/j.chaos.2005.09.046
7. V. M. Gandhimathi and S. Rajasekar, Physica Scripta **76**, 693 (2007). https://doi.org/10.1088/0031-8949/76/6/019
8. J. H. Yang and X. B. Liu, Physica Scripta **83**, ID 025006 (2010). https://doi.org/10.1088/0031-8949/82/02/025006
9. L. Ravisankar, V. Ravichandran, and V. Chinnathambi, Int. J. Eng. Sci. **1**, 17 (2012).
10. M. V. S. Meenakshi, S. Athisayanathan, V. Chinnathambi, and S. Rajasekar, Chinese J. Phys. **55**, 2208 (2017). https://doi.org/10.1016/j.cjph.2017.09.009
11. G. Duffing, Erzwungenc Schwingungen bei Vera¨nderlicher Eigenfrequenz (Braun-Schweig, 1918).
12. S. V. Priyatharsini, M. V. S. Meenakshi, V. Chinnathambi, and S. Rajasekar, J. Math. Model. **7**, 263 (2019).
13. V. Ravichandran, V. Chinnathambi, and S. Rajasekar, Pramana J. Phys. **67**, 351 (2006). https://doi.org/10.1007/s12043-006-0079-9
14. S. Sabarathinam and K. Thamilmaran, Nonlinear Dynam. **87**, 2345 (2017). https://doi.org/10.1007/s11071-016-3194-2
15. V. Varshney, S. Sabarathinam, A. Prasad, and K. Thamilmaran, Int. J. Bifurcation Chaos **28**, ID 1850013 (2018). https://doi.org/10.1142/S021812741850013X
16. C. Jeevarathinam, S. Rajasekar, and M. A. F. Sanjuan, Physical Rev. E **83**, ID 066205 (2011). https://doi.org/10.1103/PhysRevE.83.066205
17. H. G. Liu, X. L. Liu, J. H. Yang, M. A. F. Sanjuán, and G. Cheng, Nonlinear Dynam. **89**, 2621 (2017). https://doi.org/10.1007/s11071-017-3610-2
18. J. Yang, S. Zhang, M. A. F. Sanjuán, and H. Liu, Communicat. Nonlinear Sci. Numer. Simulat. **5**, ID 105258 (2020). https://doi.org/10.1016/j.cnsns.2020.105258
19. J. Cantisán, M. Coccolo, J. M. Seoane, and M. A. F. Sanjuán, Int. J. Bifurcation Chaos **30**, ID 2030007 (2020). https://doi.org/10.1142/S0218127420300074
20. S. Jeyakumari, V. Chinnathambi, S Rajasekar, and M. A. F. Sanjuán, Int. J. Bifurcation Chaos **21**, 275 (2011). https://doi.org/10.1142/S0218127411028416
21. A. Venkatesan, S. Parthasarathy, and M. Lakshmanan, Chaos, Solitons Fractals **18**, 891 (2003). https://doi.org/10.1016/S0960-0779(03)00092-4
22. V. Ravichandran, V. Chinnathambi, and S. Rajasekar, Ind. J. Phys. **86**, 907 (2012). https://doi.org/10.1007/s12648-012-0128-9
23. B. Yu Guo, Z. Reyes, A. Reyes, and A. C. J. Luo - *ASME Int. Mechinical Eng. Congress Exposition* IMECE2018-86833, V04BT06A027 (2019). https://doi.org/10.1115/IMECE2018-86833
24. L. Hou, X. Su, and Y. Chen, Int. J. Bifurcation Chaos **29**, ID 1950173 (2019), https://doi.org/10.1142/S0218127419501736
25. H. L. Koudahoun, Y. J. F. Kpomahou, J. Akande, and D. K. K. Adjaï, World J. Appl. Phys. **3**, 34 (2018). https://doi.org/10.11648/j.wjap.20180302.13
26. B. Ahmad, J. Nonlinear Dynam. **2013**, ID 824701 (2013). https://doi.org/10.1155/2013/824701
27. C. Wu, Z. Wang, J. Yang, D. Huang, and M. A. F. Sanjuán, Eur. Phys. J. Plus **135**, 130, (2020).
28. P. Jia, J. Yang, C. Wu, and M. A. F. Sanjuán, J. Vibrat. Control **25**, 141 (2019). https://doi.org/10.1177/1077546318772257
29. H. Delavari and M. Mohadeszadeh, J. Control Eng. Appl. Informatics **20**, 67 (2018).
30. A. Khan and H. Chaudhary, J. Sci. Res. **12**, 201 (2020). https://doi.org/10.3329/jsr.v12i2.43790

31. S. Rasappan and S. Vaidyanathan, Synchronization of Hyperchaotic Liu System via Backstepping Control with Recursive Feedback - *Int. Conf. on Eco-friendly Computing and Communication Systems* (Springer, 2012) pp. 212–221. https://doi.org/10.1007/978-3-642-32112-2_26
32. M. Chen and Z. Han, Chaos, Solitons Fractals **17**, 709 (2003). https://doi.org/10.1016/S0960-0779(02)00487-3
33. L. S. Jahanzaib, P. Trikha, and Nasreen, J. Sci. Res. **12**, 189 (2020). https://doi.org/10.3329/jsr.v12i2.43780
34. D. Li and X. Zhang, Neurocomputing **216**, 39 (2016). https://doi.org/10.1016/j.neucom.2016.07.013
35. F. C. Moon and P. J. Holmes, J. Sound Vibrat. **65**, 275 (1979). https://doi.org/10.1016/0022-460X(79)90520-0
36. A. Wolf, J. B. Swift, H. L. Swinney, and J. A. Vastano, Physica D **16**, 285 (1985). https://doi.org/10.1016/0167-2789(85)90011-9